

Optimization of surface pretreatment for single GaN nanowire devices

Andrew M. Herrero and Kris A. Bertness^{a)}

Quantum Electronics and Photonics Division, National Institute of Standards and Technology, Boulder, Colorado 80305

(Received 19 July 2012; accepted 11 September 2012; published 28 September 2012)

The correlation of residual contamination with void formation at the contact/SiO₂ interface for single GaN nanowire (NW) devices was investigated. The morphology of the metal/SiO₂ interface was studied by removing annealed Ni/Au films from the SiO₂ surface with carbon tape, mounting the films for scanning electron microscopy and imaging. Formation of voids at the metal/SiO₂ interface, which can negatively affect device performance, was shown to occur during annealing of Ni/Au contacts to NWs on SiO₂. It was discovered that residual contamination, both from the NW solution and from photolithographic processes on the NW-SiO₂ surface prior to metal deposition, can cause significant increases in the number of voids observed at the metal/SiO₂ interface. Various predeposition cleaning methods were investigated in order to minimize the amount of void formation associated with residual contamination. The degree of void formation at the metal/SiO₂ interface is used to evaluate the effectiveness of each cleaning method. It was determined that the most effective cleaning method for removing residual contamination from the NW-SiO₂ surface was an ultraviolet ozone treatment followed by a dilute HCl bath, immediately preceding contact deposition. [<http://dx.doi.org/10.1116/1.4754701>]

I. INTRODUCTION

GaN nanowires (NWs) are promising for a number of technical applications, including high-performance LEDs¹⁻³ and lasers^{4,5} and numerous other electronic devices.^{6,7} Optimization of device performance is dependent on the electrical characterization of single-NW devices. These single-NW devices are made by dispersing a NW solution onto an insulating substrate and forming contact pads on the substrate via conventional photolithography and metal deposition. This process results in randomly formed two-terminal, single NW devices. The insulating substrate most commonly used is a SiO₂ film on a Si wafer.^{8,9} For metals deposited on a SiO₂ surface, a common problem resulting from heat treatment is the occurrence of void formation at the metal/SiO₂ interface. Void formation can cause cracking and delamination of the metal film as well as reduce the contact area, which can increase the resistance or lead to a complete failure of the NW device. There are multiple causes of this void formation, some of which are inherent in the material system and deposition method used, while others are more controllable. A well-known cause of void formation is the presence of residual contamination on the substrate prior to metal deposition. The origin of the contamination is usually from process chemicals that were not completely removed with appropriate cleaning and pretreatment procedures.

We investigated Ni/Au films for use as ohmic contacts to our p-GaN NWs. Ni/Au contacts oxidized in N₂/O₂ atmospheres are the predominant contact scheme applied to p-GaN. The diffusion of Ni in response to oxidation improves the contact resistance and adds to the transparency of the contact.¹⁰⁻¹² In our studies, we have observed void formation after annealing the Ni/Au films, which causes severe cracking

or delamination from the SiO₂ surface and degradation in the contact performance of the NW devices. In addition to void formation, the presence of residual contamination at the metal/semiconductor interface is known to increase the barrier height at that interface, resulting in poor device performance. The effect of cleaning and pretreatment of the NWs and SiO₂ surface prior to metal deposition was investigated by removing the annealed Ni/Au film from the SiO₂ and imaging the underside with SEM to determine the amount of void formation. An optimal cleaning process was developed that removes all residual contamination caused by the NW solution and photolithography processes. This process was a combination of UV ozone treatment, widely used to remove organic contaminants from surfaces, and HCl etching, which appears to passivate the surface against reabsorption of contaminants.

II. EXPERIMENT

The GaN NWs were grown by catalyst-free molecular beam epitaxy (MBE) on Si(111) substrates. The details of the NW growth conditions were presented elsewhere.¹³ The NW solution is prepared by sonicating a piece of the as-grown sample in a solvent to free the NWs from the growth substrate. Isopropanol (IPA) and deionized water (H₂O) were used as solvents for the NW solution. The NW solution is dispersed onto a SiO₂ (200 nm)/Si wafer. In the controlled NW solution volume experiments, 30 μ l-sized drops were dispersed and expanded to cover the whole surface of the 1 cm² sample. Additional drops were deposited after the solvent from the previous drop had completely evaporated. After the final drop of NW solution had evaporated, the sample was gently dipped in successive baths of acetone and isopropanol to remove unwanted impurities, rinsed in deionized H₂O and blown dry in N₂. Standard photolithography steps were performed on some samples, which consisted of spinning on photoresist, exposing the

^{a)}Electronic mail: kris.bertness@nist.gov

entire surface (no mask), developing, rinsing with deionized H_2O , and blowing dry with N_2 . Prior to loading the samples into the electron-beam evaporator for metal deposition, different cleaning procedures were performed on the samples. Some samples received no predeposition cleaning, while others received either a 10 min UV ozone treatment with an O_2 flow rate of 80 sccm or the same UV ozone treatment followed by a 1-min $HCl:H_2O$ (1:10) bath. These treatments are labeled “UVO” and “UVO+HCl,” respectively, throughout the remainder of the paper. The thicknesses of the Ni and Au films were 50 and 100 nm, respectively. All Ni/Au films used in this study were annealed under ultra-high-purity N_2/O_2 (3:1) at $550^\circ C$ for 10 min. To view the metal/ SiO_2 interface, the Ni/Au films were peeled from the SiO_2 substrate with carbon tape, then mounted and imaged in a field-emission scanning electron microscope (FESEM). An illustration of this process is shown in Fig. 1. The area of the voided regions was deter-

mined using imaging software. The figures indicate the average void area (as a percentage of the total area). For some samples, multiple $100 \mu m^2$ areas were analyzed. The standard deviation of these data sets indicates that this method typically has errors of about $0.2 \times$ the measured value.

III. RESULTS

Removing the annealed Ni/Au films from the SiO_2 substrate allowed the underside morphology of the Ni/Au film to be studied with SEM. In Fig. 2(a), the top surface of an annealed Ni/Au contact on SiO_2 is shown. Figure 2(b) shows the underside from the same area of that particular Ni/Au film after removal from the SiO_2 surface with carbon tape. The dark spots on the surface of the Ni/Au in Fig. 2(a) coincide with the dark features on the underside of the film seen in Fig. 2(b). The most significant observation made after imaging the Ni/Au underside was the extensive voiding that had occurred in the Au layer adjacent to the SiO_2 . The general structure of the Ni/Au film on SiO_2 after annealing can be described with the illustration in Fig. 2(c), which shows that most of the Ni has diffused to the surface and formed NiO. The underlying layer is a Au-rich network with large voided regions. These voids have been observed previously and are formed by thermodynamically favored chemical reactions.^{12,14} The voided regions reduce the amount of metal/ SiO_2 interface area, which promotes cracking and delamination of the Ni/Au film.

In order to determine how much of the void formation was due to the residual contamination from the photolithography process, the first set of experiments was performed

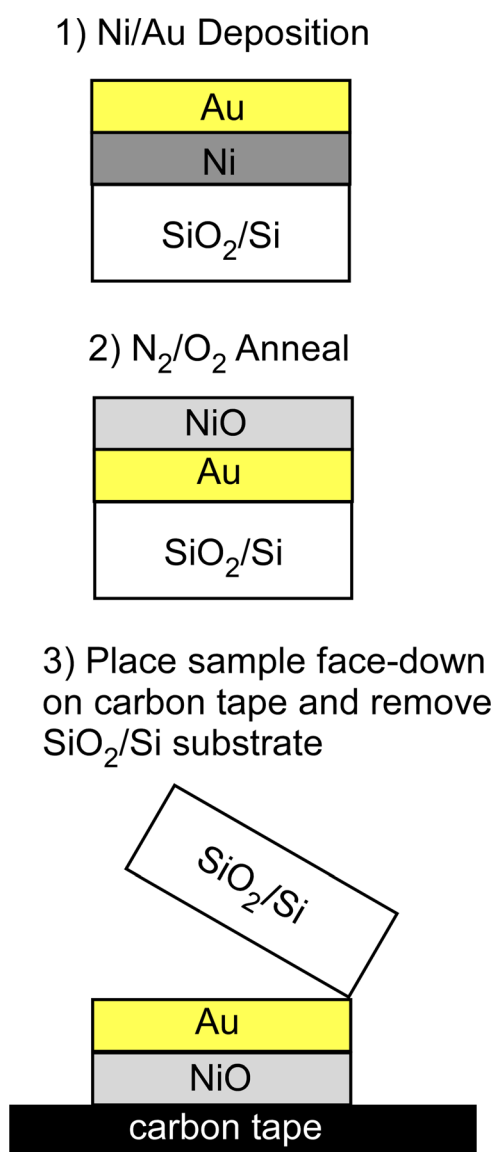


Fig. 1. (Color online) Illustration of process to remove Ni/Au films from the SiO_2/Si substrate in order to image the metal/ SiO_2 interface.

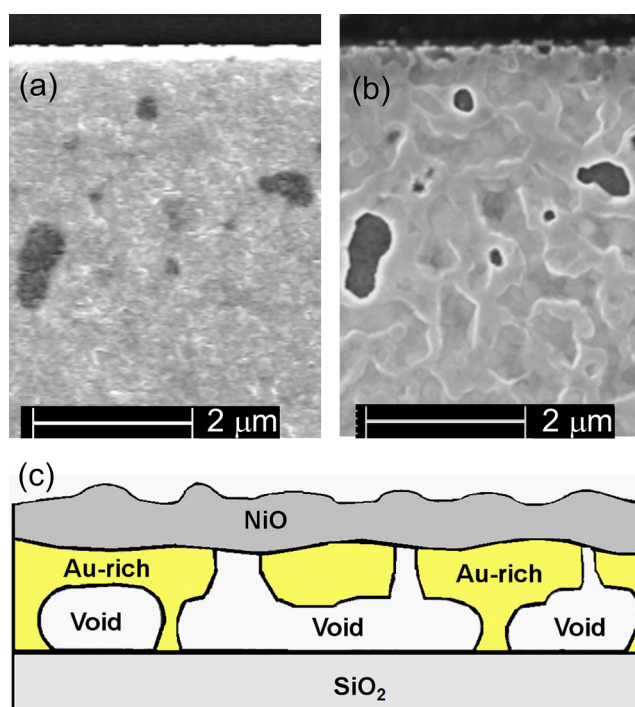


Fig. 2. (Color online) (a) SEM image of annealed Ni/Au film on SiO_2 . (b) SEM image of the underside of annealed Ni/Au film shown in (a) after removal from the SiO_2 surface with carbon tape. (c) Illustration of annealed Ni/Au film on SiO_2 in cross-section.

without applying a NW solution. These experiments focused on the effectiveness of the various predeposition cleaning methods for the removal of the residual contamination. Figures 3(a)–3(f) show the underside of six annealed Ni/Au films from this study. The samples in Figs. 3(a)–3(c) did not receive any photolithographic processing, while the samples in Figs. 3(d)–3(f) did receive photolithographic processing on the bare SiO₂ surface. Each of the three samples from both groups received a different predeposition cleaning: no predeposition cleaning, UVO pretreatment, or UVO+HCl. The effect of photolithography and the different cleaning methods on void formation is readily apparent from the images. We observed the largest degree of void formation for the SiO₂ surface that received photolithographic processing and no predeposition cleaning. For the SiO₂ surfaces that received no photolithographic treatment, the sample treated with only UV ozone had the largest amount of void formation. This is most likely due to a change in the chemical nature of the SiO₂ surface and not from additional contamination, as detailed in Sec. IV. Both the UVO and the

UVO+HCl treatments resulted in a reduction in the amount of residue from photolithographic processes, but the UVO+HCl treatment showed a much more significant reduction in photolithographic residue. In Fig. 3(g), the calculated void areas (as a percentage of the total area) are plotted for each sample shown in Figs. 3(a)–3(f). Both samples that received the UVO+HCl pretreatment were observed to have approximately the same low void area, confirming that any residue from the photolithography process was completely removed.

The next set of experiments examined whether the type of solvent in the NW solution affects void formation, specifically comparing IPA, deionized H₂O, and no NW solution. All samples in this set received photolithographic processing. The amount of void formation for samples processed with each NW solution, along with the samples processed without NW solution, is plotted in Fig. 4. As shown previously for samples processed without a NW dispersal step, the amount of void formation associated with photolithographic residue decreases with predeposition cleaning. Regardless of the type of solvent in the NW solution, void formation is minimized when the UVO+HCl pretreatment is used.

Because the typical solvent used for NW solutions is IPA,^{8,9} other effects of the IPA NW solution on void formation were investigated. The large fractional area of voids in Fig. 3(a) compared to Fig. 3(c) indicates that some contamination might be present on the SiO₂ surface prior to NW dispersal and photolithography. In order to determine whether as-received substrate contamination has any effect on void formation, some samples were processed with a UVO+HCl cleaning step for the SiO₂ substrate *prior* to NW dispersal,

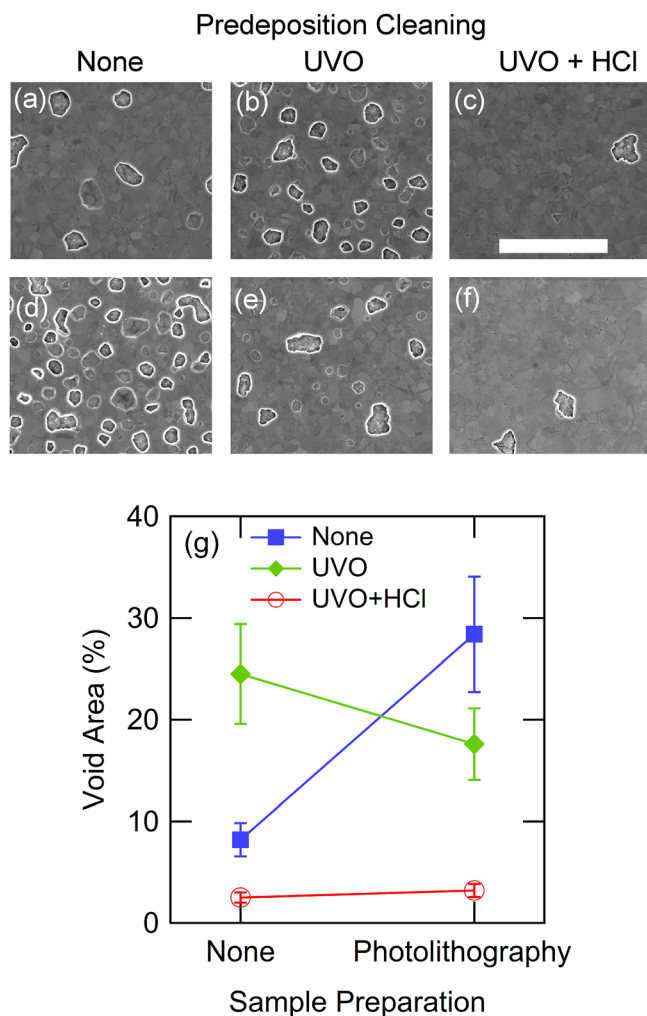


FIG. 3. (Color online) Underside of annealed Ni/Au films deposited on SiO₂ surfaces. [(a)–(c)] Samples received no photolithographic processing of SiO₂ surface prior to predeposition cleaning. [(d)–(f)] Samples received photolithographic processing prior to predeposition cleaning. (g) Plotted values of the areas of the voided regions for each sample shown in (a)–(f).

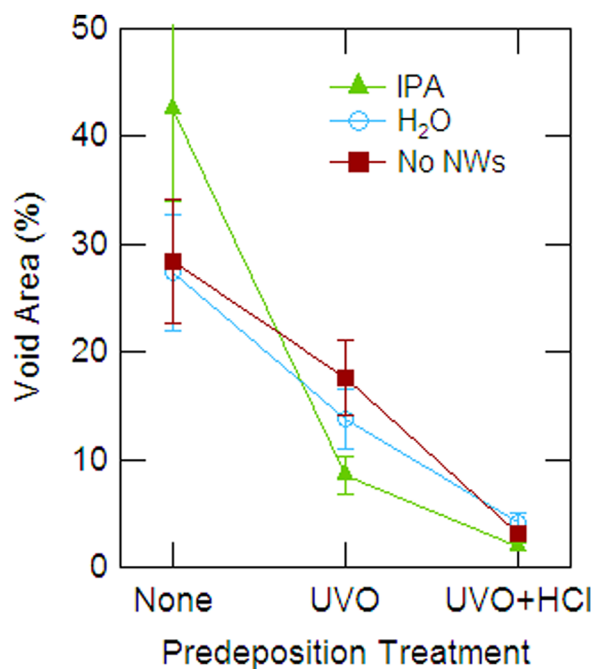


FIG. 4. (Color online) Amount of void formation (as a percentage of total area) at the annealed (Ni/Au)/SiO₂ interface for each type of NW solution and cleaning procedure used.

photolithography, and additional predeposition cleaning. As seen in Fig. 5(a), the amount of void formation is approximately the same whether the substrate received an initial cleaning treatment or not. Another issue was the effectiveness of the cleaning procedures when different amounts of NW solution were used. Samples were processed using the same cleaning and photolithographic procedures, except for the amount of NW solution that was dispersed. Figure 5(b) shows the effect of the amount of IPA NW solution on void formation. The increase in void formation is minimal when comparing less than 60 μl for each cleaning procedure. For greater amounts of IPA NW solution, there is a significant increase in void formation, particularly for the UVO treatment. The amount of IPA NW solution dispersed can there-

fore affect the amount of residual contamination that develops.

IV. DISCUSSION

The removal of annealed Ni/Au films from SiO_2/Si substrates in order to image the underside is an excellent tool for evaluating the effectiveness of different predeposition cleaning procedures. This method is relatively inexpensive and simple to perform, and the results are easy to interpret. Although the ability to remove the metal film from the SiO_2 surface is limited to metal schemes that have poor adhesion, the effectiveness of the cleaning procedures applies to the deposition of any metal film on SiO_2 .

The samples processed without NW solution clearly show the existence of residual contamination from photolithographic processes. For the samples processed with different NW solutions, only the IPA NW solution appears to leave residue on the SiO_2 surface after dispersal. The amount of residue is dependent on the amount of IPA NW solution that is allowed to evaporate on the SiO_2 surface. The increase in void formation for IPA NW solution volume greater than 60 μl is most likely due to incomplete removal of the residue. The residue from the photolithography and the IPA NW solution is reduced when the NW- SiO_2 surface receives a UVO treatment. Complete removal of the contamination is only accomplished with the UVO+HCl treatment.

Although the type of NW solution and cleaning procedure both had a clear effect on the amount of void formation between the metal and SiO_2 , the void formation around the NW does not appear to be influenced by these factors. Shown in Figs. 6(a) and 6(b) are NWs embedded in an annealed Ni/Au film after receiving the UVO+HCl pretreatment and the UVO pretreatment, respectively. Despite the large difference in void formation at the metal/ SiO_2 interface for the different pretreatments, the void formation around the NW is very similar. The origin of the void formation directly around the NW is most likely associated with the 3D morphology of the NW and the deposition method. Figure 6(c) shows a NW embedded in an as-deposited Ni/Au film. The arrows in the picture point out the small gaps in the metal on either side of NW that form because of shadowing during the electron-beam evaporation. Figure 6(d) is an illustration of the as-deposited NW contact structure showing the gaps. These gaps most likely act as sinks for voids, which increases the void concentration around the NW.

We have considered the possibility that the HCl may be prevented from reaching the nanowire lower facets by liquid surface tension or that the NW acts as a collection point for contamination because liquids tend to evaporate last around the NW. The UVO treatment, based on gas flow, would not be affected by the geometry. To test these hypotheses, we performed two control experiments. In the first experiment, the nanowires were transferred to the substrate with a dry transfer method (scraping the as-grown piece across the SiO_2) and covered with Ni/Au without any photolithography step. Some of these specimens were cleaned with UVO only before Ni/Au evaporation and others were not. In the second control

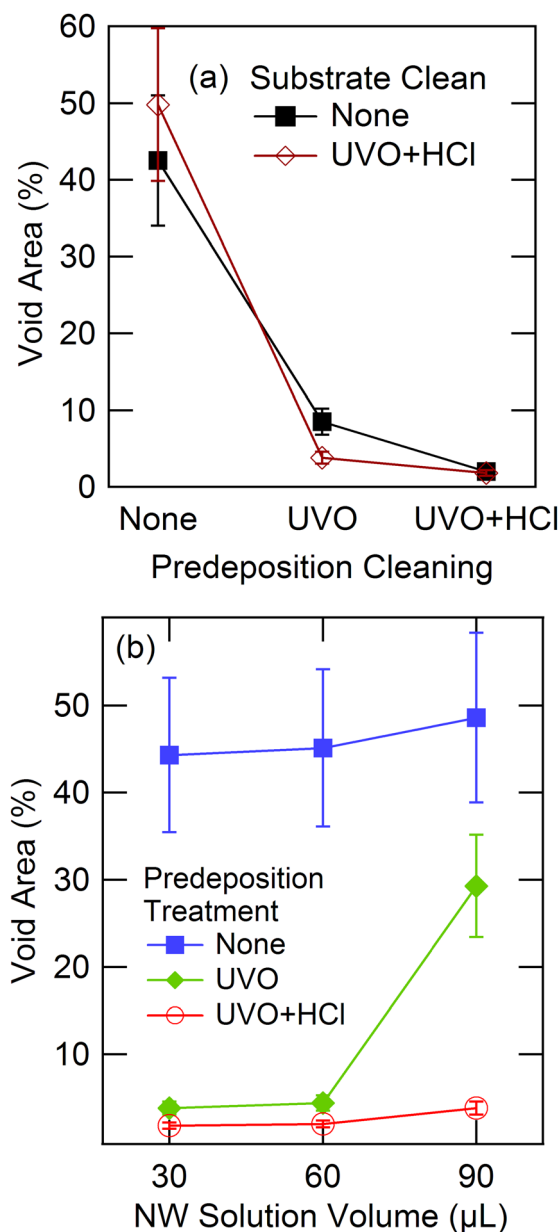


Fig. 5. (Color online) (a) Effect of as-received SiO_2 substrate clean prior to NW dispersal and photolithography on the amount of void formation at the annealed (Ni/Au)/ SiO_2 interface. (b) Effect of amount of NW solution used on void formation at the annealed (Ni/Au)/ SiO_2 interface.

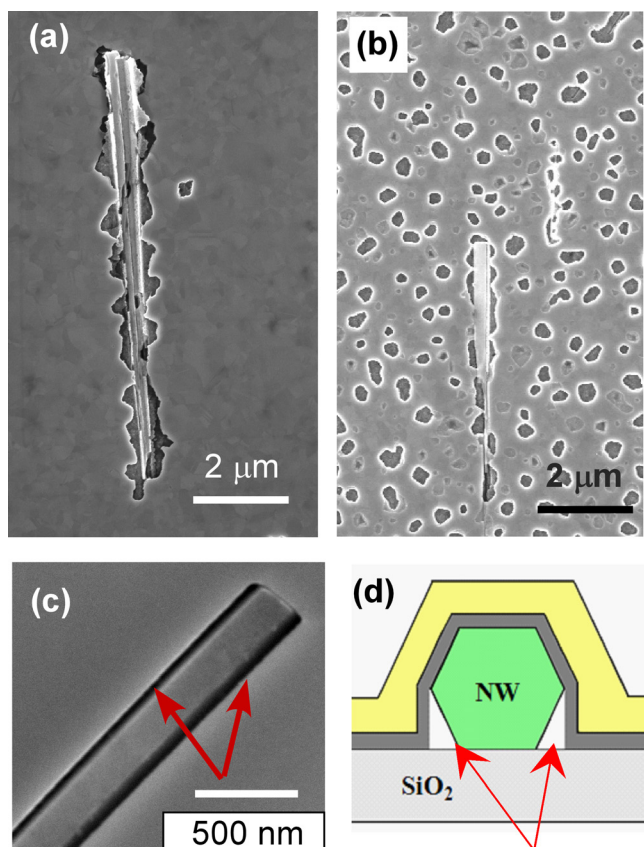


Fig. 6. (Color online) NWs embedded in an annealed Ni/Au film that received a predeposition cleaning of (a) UVO+HCl and (b) UVO only. (c) NW embedded in an as-deposited Ni/Au film. (d) Illustration of as-deposited NW contact structure.

experiment, the nanowires were dispersed in IPA, covered with photoresist, and cleaned with the UVO+HCl process modified by the addition of a soap treatment just prior to the HCl etch. The soap serves to reduce surface tension and subsequent exclusion of liquids from small trenches, in this case, the volume between the lower facets of a NW and the substrate. In all cases, the extensive void formation around the NWs persisted to the same degree seen in Fig. 6.

As mentioned above, the increase in void area for the UVO-treated SiO_2 surface that received no photolithographic treatment [Fig. 3(b)] is possibly explained by the lower initial amounts of contamination on the surface, which led to greater interaction between the ozone and the SiO_2 surface. Previous studies have shown that UV ozone removes the contaminants from the SiO_2 surface, leaving unstable dangling bonds that become terminated with hydroxyl ($-\text{OH}$) groups, making the SiO_2 surface more hydrophilic and thus susceptible to adsorption of contaminants.^{15–17} This mechanism also explains the increased effectiveness of the cleaning procedure that includes both the UV ozone treatment and the HCl bath. By following the

UV ozone treatment with an HCl bath, Cl ions replace the hydroxyl groups, leaving the surface hydrophobic. The same principle applies to the use of silanes as adhesion promoters on SiO_2 for photolithographic processes.^{18–22}

V. SUMMARY

Methods of predeposition cleaning and NW dispersal for single GaN NW devices were investigated in order to minimize residual contamination of the NW- SiO_2 surface. The effectiveness of the different cleaning methods was evaluated by studying the degree of void formation at the metal/ SiO_2 interface. Photolithography and the use of IPA as the solvent for a NW solution were shown to leave residue on the NW- SiO_2 surface, which increased the void formation at the metal/ SiO_2 interface. Complete removal of the residual contamination from the NW- SiO_2 surface was achieved by the use of a UV ozone treatment, followed by a dilute HCl bath. The HCl bath is believed to be necessary in order to inhibit contamination of the surface after cleaning.

¹A. Kikuchi, M. Kawai, M. Tada, and K. Kishino, *Jpn. J. Appl. Phys., Part 2* **43**, L1524 (2004).

²H. M. Kim, Y. H. Cho, H. Lee, S. I. Kim, S. R. Ryu, D. Y. Kim, T. W. Kang, and K. S. Chung, *Nano Lett.* **4**, 1059 (2004).

³Z. Zhong, F. Qian, D. Wang, and C. M. Lieber, *Nano Lett.* **3**, 343 (2003).

⁴J. C. Johnson, H. J. Choi, K. P. Knutse, R. D. Schaller, P. Yang, and R. J. Saykally, *Nature Mater.* **1**, 106 (2002).

⁵J. Ristic, E. Calleja, S. Fernandez-Garrido, A. Trampert, U. Jahn, K. H. Ploog, M. Povoloskiy, and A. Di Carlo, *Phys. Status Solidi A* **202**, 367 (2005).

⁶E. Stern *et al.*, *Nanotechnology* **16**, 2941 (2005).

⁷P. T. Blanchard, K. A. Bertness, T. E. Harvey, L. M. Mansfield, A. W. Sanders, and N. A. Sanford, *IEEE Trans. Nanotechnol.* **7**, 760 (2008).

⁸W. Lu and C. M. Lieber, *J. Phys. D: Appl. Phys.* **39**, R387 (2006).

⁹M. Law, J. Goldberger, and P. Yang, *Annu. Rev. Mater. Res.* **34**, 83 (2004).

¹⁰D. Qiao, L. S. Yu, S. S. Lau, J. Y. Lin, H. X. Jiang, and T. E. Haynes, *J. Appl. Phys.* **88**, 4196 (2000).

¹¹Z. Z. Chen, Z. X. Qin, Y. Z. Tong, X. D. Hu, T. J. Yu, Z. J. Yang, X. M. Ding, Z. H. Li, and G. Y. Zhang, *Mater. Sci. Eng. B* **100**, 199 (2003).

¹²C. Y. Hu, Z. B. Ding, Z. X. Qin, Z. Z. Chen, K. Xu, Z. J. Yang, B. Shen, S. D. Yao, and G. Y. Zhang, *J. Cryst. Growth* **298**, 808 (2007).

¹³K. A. Bertness, A. Roshko, N. A. Sanford, J. M. Barker, and A. V. Davydov, *J. Cryst. Growth* **287**, 522 (2006).

¹⁴L.-C. Chen, J.-K. Ho, F.-R. Chen, J.-J. Kai, L. Chang, C.-S. Jong, C. C. Chiu, C.-N. Huang, and K.-K. Shih, *Phys. Status Solidi A* **176**, 773 (1999).

¹⁵C. L. Fan, Y. Z. Lin, and C. H. Huang, *Semicond. Sci. Technol.* **26**, 045006 (2011).

¹⁶N. S. McIntyre, R. D. Davidson, T. L. Walzak, R. Williston, M. Westcott, and A. Pekarsky, *J. Vac. Sci. Technol. A* **9**, 1355 (1991).

¹⁷R. K. Iler, *The Chemistry of Silica*, 2nd ed. (Wiley Interscience, New York, 1979).

¹⁸L. L. Chua, J. Zausmell, J. F. Chang, H. Siringhaus, and R. H. Friend, *Nature* **434**, 194 (2005).

¹⁹P. Raghu, N. Rana, C. Yim, E. Shero, and F. Shadman, *J. Electrochem. Soc.* **150**, F186 (2003).

²⁰O. Sneh, M. A. Cameron, and S. M. George, *Surf. Sci.* **364**, 61 (1996).

²¹O. Sneh and S. M. George, *J. Phys. Chem.* **99**, 4639 (1995).

²²D. W. Sindorf and G. E. Maciel, *J. Am. Chem. Soc.* **105**, 1487 (1983).